



Article

In Vivo Complete-Arch Implant Digital Impressions: Comparison of the Precision of Three Optical Impression Systems

Jaime Orejas-Perez ¹, Beatriz Gimenez-Gonzalez ², Ignacio Ortiz-Collado ¹, Israel J. Thuissard ³
and Andrea Santamaria-Laorden ^{1,*}

¹ Faculty of Biomedical and Health Sciences, Department of Clinical Dentistry, Universidad Europea de Madrid, 28670 Madrid, Spain; jaime.orejas@universidadeuropea.es (J.O.-P.); ignacio.ortiz@universidadeuropea.es (I.O.-C.)

² Department of Implantology and Prosthetic Dentistry, Academic Center for Dentistry Amsterdam ACTA, 1081 LA Amsterdam, The Netherlands; b.gimenezgonzalez@acta.nl

³ Faculty of Biomedical and Health Sciences, Department of Medicine, Universidad Europea de Madrid, 28670 Madrid, Spain; israeljohn.thuissard@universidadeuropea.es

* Correspondence: andrea.santamaria@universidadeuropea.es

Abstract: (1) Multiple in vitro studies reported insufficient accuracy of intraoral scanners (IOSs) for complete-arch multiple implant impression. The aim of the study is to analyze the precision of three IOSs, PIC dental (Pic dental, Iditec North West SL), TRIOS 3 (3Shape), and True Definition (Midmark Corporation) and the influence of several factors in the edentulous complete maxillary and mandibular arch. (2) A fully edentulous patient with eight implants in the maxillary and in the mandibular jaw was selected. Five impressions were taken per system and arch. A suprastructure was designed on each digital working cast. The precision was analyzed comparing each of the 28 distances and seven relative angulations of the abutments of all the designed suprastructures. The descriptive statistics, the Student's *t*-test, and the ANOVA test were used to analyze the data ($\alpha = 0.05$). (3) Significant differences were observed when comparing the IOSs in some of the distances and angulations. (4) The increase in the distance between implants affected the precision of T and TD but not the PIC system. The type of arch did not affect the PIC precision, but the T and TD systems performed worse in the mandibular arch. The system with the best precision was the PIC, followed by TD, and then T.

Keywords: optical impression; intraoral scanners; edentulous; complete arch; dental implants; precision



Citation: Orejas-Perez, J.; Gimenez-Gonzalez, B.; Ortiz-Collado, I.; Thuissard, I.J.; Santamaria-Laorden, A. In Vivo Complete-Arch Implant Digital Impressions: Comparison of the Precision of Three Optical Impression Systems. *Int. J. Environ. Res. Public Health* **2022**, *19*, 4300. <https://doi.org/10.3390/ijerph19074300>

Academic Editors: Daniele Garcovich, Alfonso Alvarado Lorenzo and Fawad Javed

Received: 22 February 2022

Accepted: 31 March 2022

Published: 3 April 2022

Publisher's Note: MDPI stays neutral with regard to jurisdictional claims in published maps and institutional affiliations.



Copyright: © 2022 by the authors. Licensee MDPI, Basel, Switzerland. This article is an open access article distributed under the terms and conditions of the Creative Commons Attribution (CC BY) license (<https://creativecommons.org/licenses/by/4.0/>).

1. Introduction

The majority of studies that evaluate IOSs are performed in vitro and, therefore, lack the challenges that the IOSs face in vivo [1–5]. Despite having less clinical relevance, in vitro studies help to develop protocols and to analyze parameters that are not possible in vivo, such as accuracy [6–8]. The heterogeneity of these study designs makes the interpretation of the conclusions and clinical recommendations difficult [1,9–11].

The different IOSs in the market compete to achieve the best accuracy, defined as how closely the obtained measurements resemble the real arch measurements, and the best precision, defined as how similar the obtained measurements of the repeated scans are. (ISO 5725) [12]. Evaluating the precision in vivo is key, because there are many factors that can affect the result in the clinical setting, making the outcomes inconsistent and therefore difficult to predict. A large challenge is that there is no consensus regarding the range of acceptable misfit and the way to correctly measure the misfit clinically [9,13–17]. When the number of implants in the same structure increases, the tolerance of the error in the axis (X, Y, Z) and the angulations decrease [18]. Furthermore, we must consider the manufacturing

tolerance of the suprastructures that can generate misfits in form of GAPS between 20 and 100 microns [19,20].

The majority of the literature agrees, that in order to perform complete arch implant impressions, the conventional techniques are superior to the digital ones [3,21–26]. The hardware and software technology used by the IOSs to capture images, the scan protocol used, the algorithms needed to create the STL file, and the transformation of the STL on the 3D working cast affect the definitive result [2,27–33]. Other factors such as the mouth opening of the patient, the size of the tip, the ambient light, light reflection, saliva, steam, the number and 3D position of the scan bodies, the manufacturing material of the scan bodies, the distance between them, and the length of the edentulous span and arch length are also described as factors that affect this technology [2,34–37].

Despite several IOSs not including complete arch implant impressions in their official indications, many articles evaluate that possibility. There are several factors affecting the accuracy and precision of the IOSs, long edentulous spans (lacking references), mobile tissues, number of implants, the stitching of the 3D images to produce the STL file, which is more challenging with the anatomy of the scan bodies and edentulous spans [14,27,38–40]. This is true for all the IOSs in the market in different measures, two of which are analyzed in this study, Trios (T) and True Definition (TD) [41,42]. However, the third scanner used in this study was PIC Dental (PIC), which was specifically designed for complete arch multiple implant impressions, adapting the stereophotogrammetry technology to the oral cavity [43–48].

More *in vivo* studies are needed in order to analyze these systems in real clinical situations [1]. Comparing these results with those of the *in vitro* studies will help understand the impact of the oral environment and the real idea of the possible indications of each IOSs [1].

The aims of this *in vivo* study are: (1) to analyze the precision of the three IOSs and compare them using arbitrary limits of 75 microns per span and 0.6 degrees of angulation for each scan body, (2) to evaluate the effect of the increasing distance between the implants, from the first scanned implant to the eighth implant measuring the Euclidean distances and relative angulations, and (3) to evaluate the effect of the arch (maxillary or mandibular) in the precision of the different scanners. Therefore, the corresponding null hypotheses are: H01 There are no differences in precision between the three IOSs using the established limits as a reference. H02 The increase in distance does not affect the precision of the three IOSs. H03 The precision of the IOSs is not affected by the type of arch (maxillary or mandibular).

2. Material and Methods

Overview: Three digital impression systems were evaluated in the present study; PIC dental (PIC), Trios (T), and True Definition (TD). For this, 5 impressions were taken per arch and system in one patient with 8 implants in each arch. Every STL was transformed in its corresponding digital working cast (Figure 1). A total of 30 digital suprastructures were designed. The Euclidean distances and angulations of the scan bodies were the analyzed variables. The measurements were performed in the design of the suprastructures [14,49,50] (Figure 2).

For the study, a 65-year-old male patient classified as ASA 2, fully edentulous with 8 external hex implants with platform 4,1 and 5 mm (Medical Precision Implants MPI, Madrid, Spain) in each arch was selected. The Regional Medical Ethical committee approved the study on 7 October 2014, with the code TESISIMPLAN2014, with version 2.0, 26 September 2014. Subsequently, the Research Committee of the European University of Madrid (UEM) issued the approval on 17 November 2014 with the code CIPE/009/14.

The null hypotheses of the study were: H01 There are no differences in precision between the 3 IOSs using the established limits as a reference. H02 The increase in distance does not affect the precision of the 3 IOSs. H03 The precision of the IOSs is not affected by the type of arch (maxillary or mandibular). Assuming a 20% probability of improvement in

accuracy (alternative hypothesis), it was calculated that 5 repetitions for each impression, technique and arch on one patient were necessary to detect the clinically minimal relevant effect (OR = 1.5) with a confidence level of 95% and a statistical power of 80%.

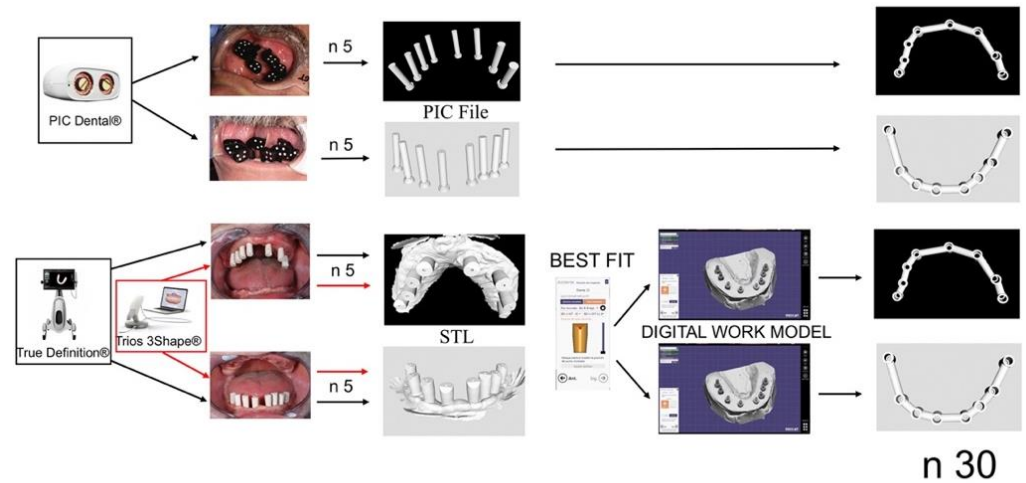


Figure 1. Diagram representing the study design. Three IOSs systems, 5 scans per arch, maxillary mandibular, digital study model, and suprastructure design.

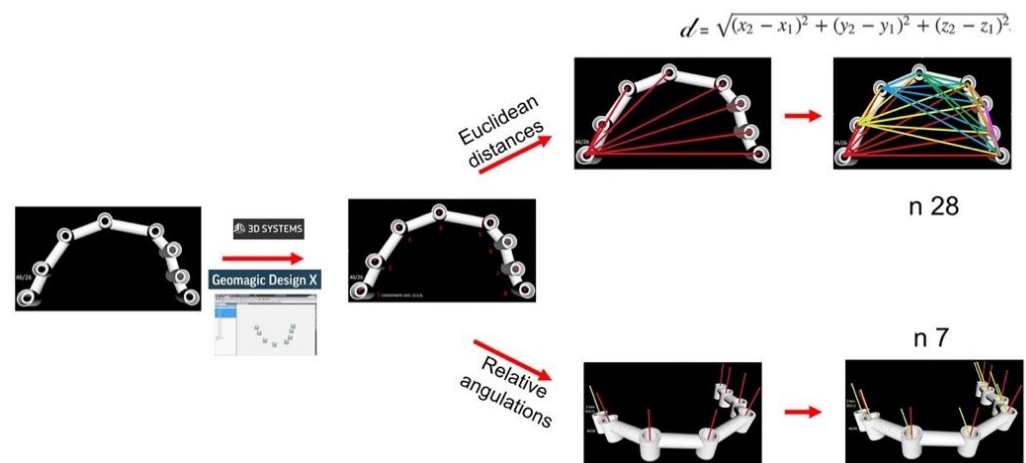


Figure 2. With reverse engineering software, center points and rotational axis of abutments are calculated for 30 designed suprastructures. From each suprastructure 28 Euclidean distances and 7 relative angulations were analyzed.

2.1. Impression Systems and Impression Techniques

The impression taking was randomized using the statistical epidemiological program (EPIDAT 3.1). Each day an impression was taken per system and arch. The impressions with the systems T and TD were taken with the same scan bodies placing them only once to avoid the effect of that step. The first impression was always taken with T because it did not need a powder spray.

2.2. PIC Dental

Impressions: Position Implants Correctly dental (Iditec North West SL) The system was created specifically to capture multiple implants intraorally. The technology is based on stereophotogrammetry. The PIC Camera registers the implants placed in the oral cavity with its software (PIC pro) (Pic dental, Iditec North West SL) and the specific and distinct identification of the scan flags named PIC Transfers. This produces a file (PIC File) in real time with the relative scan distances and angulations of the implants. The PIC Transfers were

manufactured for this study and placed by the same operator with manual torque, making sure that there was correct visibility for the camera lenses [51].

2.3. Trios 3 Pod 3Shape (T)

Impressions: Trios (3Shape A/S Copenhagen, Denmark) The system uses the technology named parallel confocal microscopy [8]. Eight scan bodies were used “Elos Accurate 6A-B Scan Body” Brånemark System RP (REF IO 6A-B; LOT 125149), along with the corresponding screwdriver “Elos Accurate IO Driver Short” (REF C13485) ELOS MEDTECH dental (Pinol A/S, Gørløse, Denmark) with 10 Nm [7].

2.4. True Definition (TD)

Impressions: Midmark (Midmark Corporation, Dayton, OH, USA). The technology used is called active wavefront sampling (AWS) and uses a titanium dioxide powder coating. The same scan bodies as with T were used, (ELOS) [7].

The impressions were taken at the University Clinic of the UEM by the same operator with more than 3 years of experience with the systems. The scanning protocols followed the instructions of the manufacturer starting always in implant 46 for the mandibular arch and 16 for the maxillary arch for T and TD. Some modifications were needed in the scanning with T and TD in order to be able to finish the impressions due to errors in the stitching of the scan bodies.

2.5. Digital Working Casts

The impressions obtained by T and TD were transformed into the digital working cast by aligning with the best fit algorithm the scan bodies with the equivalent CAD design from the implant library of the EXOCAD (EXOCAD 2.0.0.0 GmbH, Darmstadt, Germany) This step was not necessary with the PIC system, as described previously (Figure 1).

With the aim to reach the definitive step of the CAD workflow, a suprastructure was designed for each digital working cast with Exocad [52]. Each suprastructure contained 8 rotatory abutments and 7 Ackerman segments with 3 mm sections. There was no virtual space between the suprastructure and the implant; hence, the position and the results are not affected. Both steps were performed by the same operator.

2.6. Assessment of the Distances and Angulations

The designed suprastructure ($n = 30$) was exported in STL format to a reverse engineering software, Geomagic (Geomagic Inc., 3D Systems, Morrisville, NC, USA) [52]. The central points of each abutment platform were calculated ($n = 8$). The vector that passes through those points following the rotational axis of each abutment was calculated as well. The Euclidean distances were calculated connecting the central points between the segments, creating all possible combinations per suprastructure ($n = 28$). The relative angulations were calculated in degrees using the vectors of each abutment. The axis (0, 0, 0) was selected in the abutments corresponding to implant 46 in the mandibular arch and 16 in the maxillary arch. That same abutment was determined as (0, 0, 1) to calculate the angulations; in this way, abutments 46 and 26 were the reference to calculate the 7 remaining angulations (Figure 2). The Euclidean distances and angulations were calculated individually (one by one).

Due to the lack of consensus regarding the tolerable limits of misfit between the abutments and their angulations, and in order to help interpret the data, a limit of 75 microns per segment and 0,6 degrees, based on the available literature, were used to compare the precision [53,54] (Figure 3).

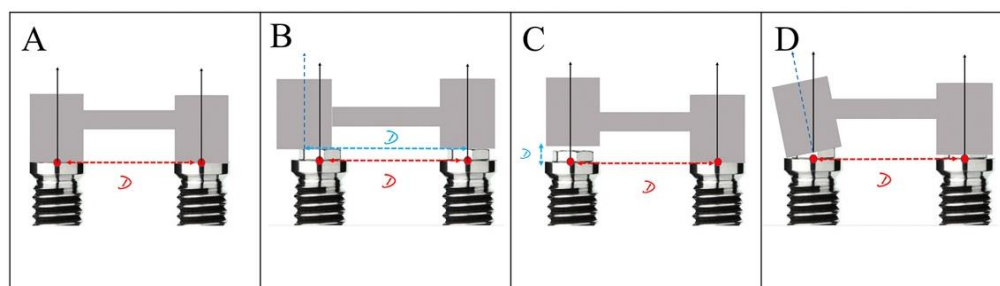


Figure 3. Representation of fit of suprastructure over two implants. (A) Ideal passive fit. (B) Misfit due to deviation on X axis between abutments. (C) Misfit due to deviation on Y axis between abutments. (D) Misfit due to variation of angulation between abutments, depending on the number of abutments involved in each prosthetic structure.

2.7. Statistical Analysis

A descriptive analysis of the data was carried out using the mean, standard deviation (SD), and maximum and minimum deviation of the distances and angulations of the abutments after the parametric behavior of the variables using the Shapiro–Wilk test was verified. The existence of statistically significant differences in the distances and angulations for the different intraoral scanners used was analyzed by means of the parametric Student’s t- and ANOVA tests, in which the Bonferroni adjustment techniques were applied for multiple comparisons.

For each system used, the variability of the measurements for the different distances and angulations was analyzed using Levene’s test of homogeneity of variances.

All the analyses were performed two-tailed, considering a significant *p*-value when it was below the alpha error (*p* < 0.05). Statistical analysis was carried out using the IBM SPSS statistics version 23.0 program (IBM Corp., 2021, Armond, NY, USA).

3. Results

The parameters, including the mean error, the standard deviation, and the minimum and maximum values, of each of the 28 distances studied for each suprastructure are shown for the maxillary in Table 1 and for the mandibular in Table 2.

Table 1. Descriptive statistics for each of 28 Euclidean distances (µm) of maxillary arch obtained by the three evaluated systems.

Euclidean Distances	PIC Dental			TRIOS			True Definition					
	Mean Error	DS	Min	Max	Mean Error	DS	Min	Max	Mean Error	DS	Min	Max
1-2	38.66	22.40	10.09	74.39	38.66	22.40	10.09	74.39	22.55	15.56	1.11	38.72
1-3	51.00	29.15	12.20	99.64	24.96	13.70	6.88	51.57	27.91	16.00	3.11	50.97
1-4	48.91	33.63	9.96	103.11	36.74	23.76	8.23	76.21	29.36	20.63	1.44	58.26
1-5	46.61	29.91	8.17	107.68	61.68	42.37	5.46	144.90	38.85	24.90	4.72	68.64
1-6	41.01	31.38	1.39	96.99	49.37	29.42	7.50	94.53	65.86	42.58	9.04	139.20
1-7	29.16	24.86	4.52	66.98	81.58	46.48	11.07	157.96	130.45	71.44	32.47	264.42
1-8	32.03	19.63	4.02	64.59	66.79	51.68	1.75	156.86	166.46	99.60	18.19	342.97
2-3	30.36	22.68	2.68	62.16	46.06	30.83	1.00	79.75	7.59	4.61	0.06	7.64
2-4	33.57	21.02	5.93	60.66	60.55	40.37	6.26	139.88	31.62	16.80	12.59	61.52
2-5	18.71	10.92	0.92	38.34	92.26	56.15	28.09	196.17	35.33	22.33	1.48	70.26
2-6	30.47	20.66	3.13	55.91	58.59	38.51	4.77	134.01	43.91	40.78	2.85	104.28
2-7	26.63	16.52	1.25	51.75	92.09	53.67	5.75	174.30	102.06	65.73	3.75	234.75
2-8	23.56	16.54	2.16	53.79	61.35	49.19	4.99	138.72	137.89	88.67	15.17	310.05
3-4	30.79	18.65	9.47	64.31	39.45	22.31	8.64	79.50	29.33	17.62	6.49	59.88
3-5	29.67	23.21	1.35	64.08	75.82	46.83	14.01	152.16	17.85	11.41	0.36	37.26
3-6	20.57	12.55	4.08	42.30	55.39	34.05	4.33	108.86	183.60	14.97	2.87	41.14

Table 1. *Cont.*

Euclidean Distances	PIC Dental				TRIOS				True Definition			
	Mean Error	DS	Min	Max	Mean Error	DS	Min	Max	Mean Error	DS	Min	Max
3-7	11.73	7.66	0.96	24.03	113.98	63.95	19.53	220.65	64.66	41.65	9.56	142.33
3-8	20.34	12.60	0.78	35.59	69.45	53.29	11.21	152.02	90.89	68.66	6.08	204.10
4-5	27.77	18.78	3.93	51.83	83.99	49.65	11.95	174.90	37.40	23.68	0.74	73.38
4-6	30.09	20.03	2.74	70.06	83.35	50.80	6.04	150.46	35.78	21.94	12.07	76.11
4-7	25.13	22.66	1.57	55.60	120.00	85.52	1.48	205.40	20.87	14.14	1.89	43.97
4-8	44.00	27.74	6.11	88.36	32.73	21.39	5.96	71.14	28.50	18.29	0.03	63.90
5-6	39.68	29.49	2.25	71.89	32.94	21.18	5.57	64.65	39.69	38.07	1.98	96.83
5-7	24.96	14.53	4.64	54.94	69.03	38.51	13.09	128.26	44.27	38.81	0.92	106.74
5-8	33.62	23.11	4.37	77.31	45.72	32.25	6.44	98.08	36.86	24.38	6.46	85.65
6-7	23.46	14.05	2.78	50.71	68.95	41.06	11.55	125.95	145.19	8.84	2.06	29.40
6-8	50.77	31.85	16.86	108.26	48.24	32.41	0.45	89.80	11.86	6.84	2.97	22.63
7-8	26.74	18.42	1.41	56.51	101.62	60.48	21.32	193.56	18.74	11.61	0.04	41.98

Standard Deviation (DS); Minimum (Min); Maximum (Max).

Table 2. Descriptive statistics for each of 28 Euclidean distances (μm) of mandibular arch obtained by the three systems evaluated.

Euclidean Distances	PIC Dental				TRIOS				True Definition			
	Mean Error	DS	Min	Max	Mean Error	DS	Min	Max	Mean Error	DS	Min	Max
1-2	15.98	11.06	1.27	29.71	29.53	16.38	7.05	61.41	39.50	23.74	4.58	82.39
1-3	34.98	20.66	8.34	66.59	12.06	11.42	0.62	27.14	20.91	13.12	1.16	40.58
1-4	14.10	11.63	2.73	31.74	29.01	18.12	4.14	52.25	31.99	17.96	5.31	64.68
1-5	23.63	21.14	2.15	55.70	82.89	48.36	6.95	166.68	46.27	26.65	15.93	98.79
1-6	33.24	18.00	11.54	66.76	118.42	68.95	6.94	246.55	53.58	33.25	7.70	118.95
1-7	18.96	11.62	0.04	36.33	149.41	86.95	40.46	316.54	82.16	68.64	1.84	18.63
1-8	26.74	14.91	9.04	53.20	203.70	138.40	20.51	476.46	111.76	123.75	3.50	269.08
2-3	44.45	26.88	7.20	98.68	19.32	10.91	5.28	40.92	10.70	7.87	1.29	24.91
2-4	34.40	19.40	4.77	64.78	28.85	26.24	0.22	64.92	13.70	8.77	2.02	26.71
2-5	35.43	20.47	7.80	66.01	45.41	27.42	0.57	80.32	19.22	11.05	1.76	40.94
2-6	46.56	30.68	1.46	104.43	62.60	36.29	5.60	117.66	27.52	16.94	6.00	58.96
2-7	41.31	30.58	4.81	89.50	75.76	45.95	13.00	154.74	37.50	22.31	9.21	69.78
2-8	33.59	24.81	1.63	70.92	118.31	78.34	6.12	272.59	61.95	35.90	13.09	113.61
3-4	29.37	18.53	4.39	53.76	16.45	12.81	0.31	32.04	11.91	7.34	0.85	23.44
3-5	26.64	16.64	0.78	46.29	32.71	18.24	8.18	64.78	15.15	10.05	1.19	34.03
3-6	31.79	19.51	0.69	70.99	41.32	27.42	0.38	85.19	27.13	14.98	6.29	57.39
3-7	16.35	11.26	1.28	38.18	50.19	31.22	13.95	104.19	36.90	21.05	5.78	67.82
3-8	12.29	9.76	0.69	27.76	93.91	55.71	18.11	202.69	59.43	33.09	11.54	115.61
4-5	24.76	17.72	2.53	56.63	19.69	11.49	3.73	38.22	15.21	18.25	0.21	37.79
4-6	33.46	24.36	2.54	64.97	24.85	16.96	0.04	50.67	24.62	17.71	1.41	56.66
4-7	23.47	15.82	0.26	51.82	34.49	18.91	11.32	66.25	27.84	16.60	2.37	54.90
4-8	8.88	7.27	0.59	20.64	70.98	41.74	12.17	149.44	43.58	24.41	11.61	86.01
5-6	15.79	12.22	2.77	35.79	8.37	6.09	0.44	20.29	14.48	9.95	1.13	34.13
5-7	16.68	10.10	0.20	36.40	13.52	7.48	2.65	25.55	19.11	11.77	2.05	43.23
5-8	28.67	22.08	0.63	53.81	54.79	32.93	12.74	120.29	42.24	26.37	0.40	82.73
6-7	27.36	17.76	0.82	51.37	7.75	6.39	0.25	17.07	6.06	3.74	1.08	11.47
6-8	27.34	22.44	3.86	61.37	42.87	31.96	3.73	102.98	29.88	22.46	1.16	67.12
7-8	21.31	13.25	4.76	44.49	47.89	30.94	3.86	110.73	41.13	33.35	0.00	31.17

Standard Deviation (DS); Minimum (Min); Maximum (Max).

When analyzing the precision data according to the selected arbitrary limits (75 μm for the distances and 0.6 degrees for the relative angulation of the abutments) the following results organized from best to worst were found: The percentage of distances that were below the 75 μm arbitrary limit were for maxillary and mandibular, respectively: 98.6%

and 95.4% for PIC, 90.4% and 80.0% for TD, and 77.9% and 68.2% for T. The percentage of angulations below the arbitrary limit of 0.6 degrees were; 100% and 100% for PIC, 91.4% and 81.4% for TD, and 87.1% and 55.7% for T (Table 3).

Table 3. Descriptive statistics where number of distances and angulations that were above/below the previously established limits are shown.

		Distances (µm)			Angulations (Degrees)		
		>75	<75	% < 75	>0.6	<0.6	% < 0.6
TRIOS	Maxillary	62	218	77.9	9	61	87.1
	Mandibular	89	191	68.2	31	39	55.7
True Definition	Maxillary	27	253	90.4	6	64	91.4
	Mandibular	56	224	80.0	13	57	81.4
PIC Dental	Maxillary	4	276	98.6	0	70	100
	Mandibular	13	267	95.4	0	70	100

For the TD and T systems, when the distance between the abutments increased, the error of each parameter studied increased as well, being more evident between the Euclidean distances from pillar 1 to 8 (Table 4 and Figures 4–6). In the TD system, a similar pattern was observed for both arches; however, T performed worse in the mandibular arch than in the maxillary arch. The IOS PIC was not affected by the increase in the distance between the abutments. The greatest difference between measurements for a segment in the maxillary arch (Table 1) was PIC 108.2 µm, T 220.6 µm, and TD 342.9 µm and for the mandibular arch (Table 2) PIC 104.4 µm, TD 269.0 µm, and T 476.4 µm.

Table 4. Maximum errors of distance measurements of each IOS in each arch. Distance 1-8 was selected to represent the distance that was most affected by accumulative error.

Euclidean Distance		1-2	1-3	1-4	1-5	1-6	1-7	1-8
TRIOS	Maxillary	74.4	51.7	76.2	144.9	94.5	157.9	156.8
	Mandibular	61.4	27.1	52.2	166.6	246.5	316.5	476.4
True Definition	Maxillary	38.7	50.9	58.2	68.6	139.2	264.4	342.9 +
	Mandibular	82.3	40.5	64.6	98.7	118.9	18.6	269.0
PIC Dental	Maxillary	74.3	99.6	103.1	107.6	96.9	66.9	64.5
	Mandibular	29.7	66.5	31.7	55.7	66.7	36.3	53.2

Tables 5 and 6 show the same parameters for the relative angulations of each abutment in the maxillary and mandibular bars, respectively. The PIC system was also not affected by the increase in the distance between implants. The TD system showed a certain increase in the mean error and DS in both arches as the separation between the abutments increased. The T system did not present an incremental pattern; however, the mandible presented 31.4% more data over 0.6 degrees than the maxillary (Figures 7 and 8).

The greatest difference between measurements for an abutment in the maxillary arch (Table 5) was 0.44 degrees for PIC, 1.01 degrees for TD, and 1.26 degrees for T; in the mandibular arch (Table 6), it was 0.24 degrees for PIC, 1.61 degrees for TD, and 2.57 degrees for T.

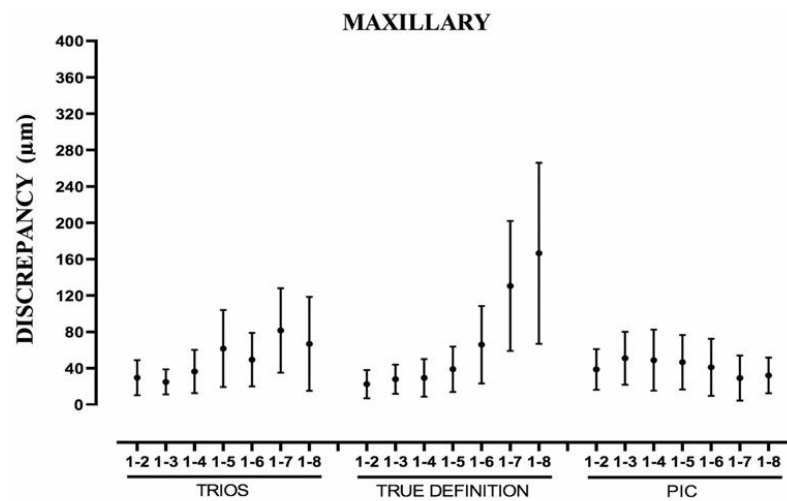


Figure 4. Boxplot showing measurements of Euclidean distances from distance 1-2 to 1-8 of maxillary arch. Point represents mean error; line represents standard deviation.

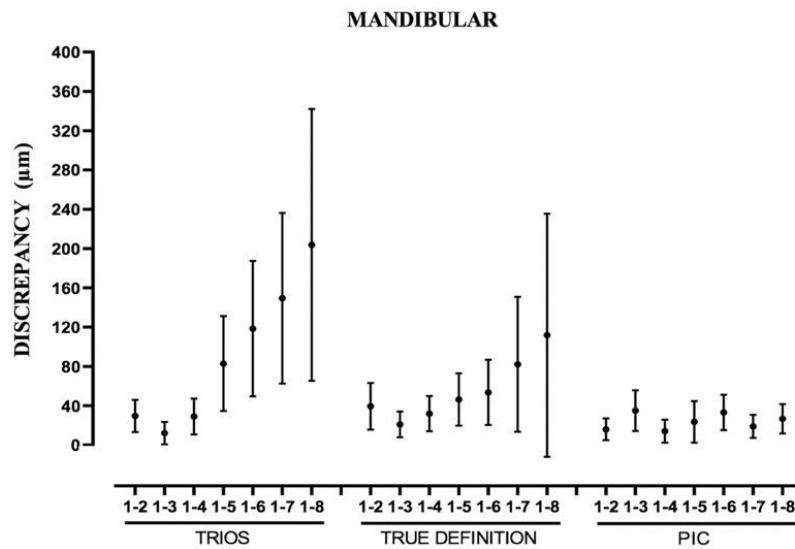


Figure 5. Boxplot showing measurements of Euclidean distances from distance 1-2 to 1-8 of mandibular arch. Point represents mean error; line represents standard deviation.

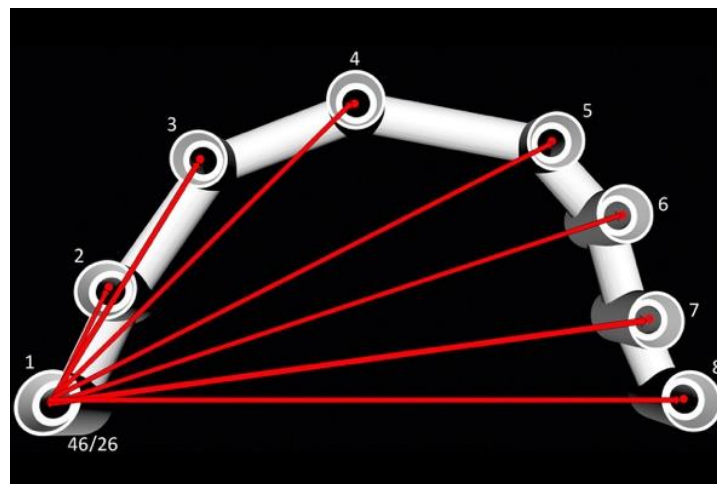


Figure 6. Representation of the Euclidean distances from abutments 1 to 8.

The distances of the 28 segments were compared between the different IOSs (PIC, T, and TD) Significant differences were found in Euclidean distances when comparing PIC–T in 14 segments for the maxillary arch and 11 for the mandibular arch. When comparing PIC–TD, 14 segments were different in the maxillary and 11 in the mandibular. Comparing TD–T, 11 segments were different in the maxillary and in the mandibular (Table 7).

Table 5. Descriptive statistics for each of seven relative angulations (degrees) of maxillary arch obtained with the three evaluated systems.

Angulation Deviations	PIC Dental				TRIOS				Angulation Deviations			
	Mean Error	DS	Min	Max	Mean Error	DS	Min	Max	Mean Error	DS	Min	Max
26	0	0	0	0	0	0	0	0	0	0	0	0
25	0.21	0.12	0.01	0.41	0.26	0.17	0.01	0.55	0.31	0.17	0.04	0.64
23	0.15	0.11	0.01	0.35	0.28	0.17	0.01	0.52	0.22	0.17	0.00	0.52
22	0.08	0.05	0.01	0.17	0.36	0.24	0.04	0.74	0.08	0.05	0.01	0.17
11	0.10	0.06	0.00	0.24	0.25	0.15	0.05	0.57	0.17	0.10	0.01	0.36
13	0.21	0.12	0.03	0.44	0.21	0.15	0.02	0.52	0.28	0.18	0.05	0.60
14	0.16	0.10	0.02	0.34	0.72	0.45	0.00	1.26	0.32	0.20	0.03	0.70
16	0.10	0.06	0.00	0.20	0.26	0.16	0.04	0.46	0.47	0.29	0.07	1.01

Standard Deviation (DS); Minimum (Min); Maximum (Max).

Table 6. Descriptive statistics for each of seven relative angulations (degrees) of mandibular arch obtained with the three evaluated systems.

Angulation Deviations	PIC Dental				TRIOS				True Definition			
	Mean Error	DS	Min	Max	Mean Error	DS	Min	Max	Mean Error	DS	Min	Max
46	0	0	0	0	0	0	0	0	0	0	0	0
45	0.08	0.05	0.00	0.20	0.53	0.55	0.02	1.25	0.08	0.05	0.01	0.17
43	0.05	0.03	0.01	0.11	0.91	0.94	0.03	2.21	0.22	0.12	0.06	0.43
42	0.04	0.03	0.00	0.09	1.05	0.95	0.05	2.49	0.28	0.24	0.00	0.62
31	0.12	0.07	0.00	0.21	1.07	0.96	0.04	2.57	0.27	0.15	0.07	0.56
33	0.03	0.01	0.00	0.06	0.32	0.20	0.07	0.73	0.41	0.25	0.04	0.72
34	0.11	0.09	0.00	0.24	0.70	0.50	0.06	1.64	0.39	0.23	0.05	0.87
36	0.10	0.60	0.02	0.19	0.86	0.57	0.12	1.99	0.77	0.45	0.24	1.61

Standard Deviation (DS); Minimum (Min); Maximum (Max).

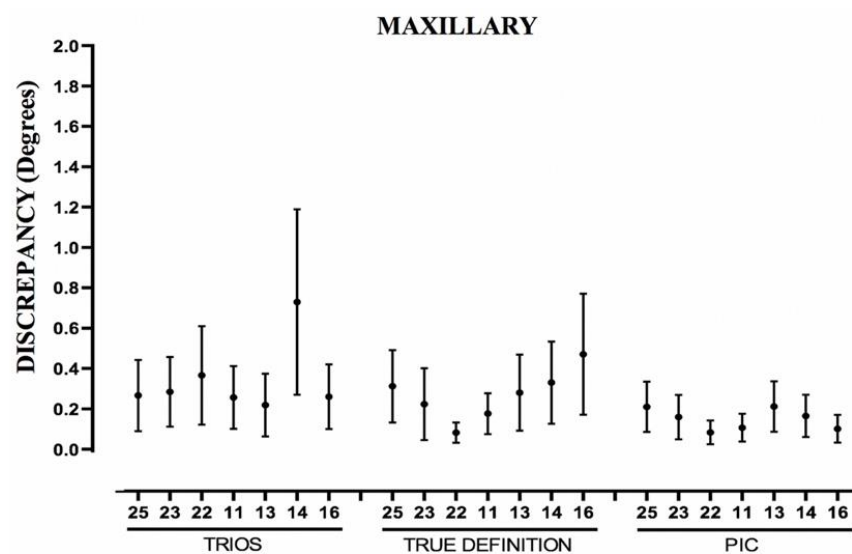


Figure 7. Boxplot showing measurements of relative angulations of abutments of maxillary arch. Abutment 26 is used as reference. Point represents mean error; line represents standard deviation.

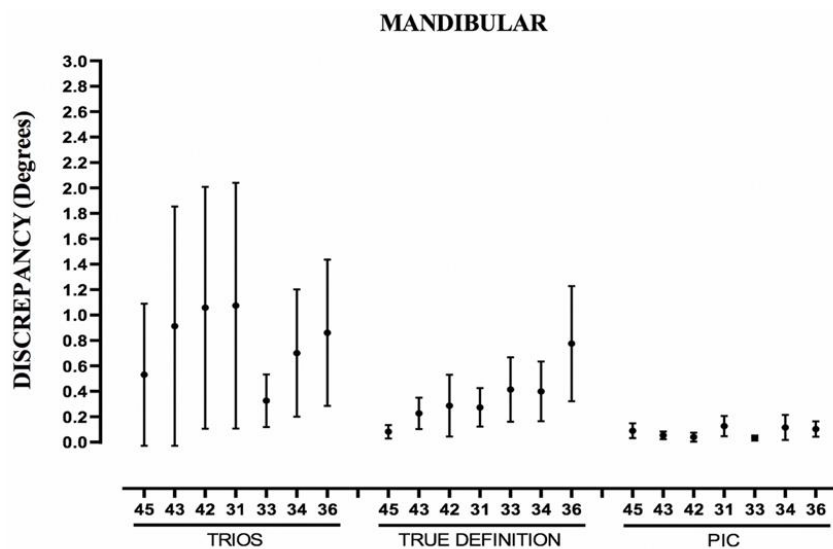


Figure 8. Boxplot showing measurements of relative angulations of abutments of mandibular arch. Abutment 46 is used as reference. Point represents mean error; line represents standard deviation.

Table 7. *p*-values of the comparisons of distance measurements between three IOSs in maxillary/mandibular arch. Significant *p*-values have been highlighted with bold numbers.

Euclidean Distances	PIC vs. TRIOS		PIC vs. Euclidean Distances		True Definition vs. TRIOS	
	Maxillary <i>p</i> -Value	Mandibular <i>p</i> -Value	Maxillary <i>p</i> -Value	Mandibular <i>p</i> -Value	Maxillary <i>p</i> -Value	Mandibular <i>p</i> -Value
1-2	0.528	0.454	0.146	0.210	0.384	0.491
1-3	0.013	0.022	0.034	0.057	0.585	0.859
1-4	0.252	0.060	0.117	0.245	0.608	0.733
1-5	0.327	0.073	0.975	0.733	0.263	0.137
1-6	0.662	0.012	0.528	0.092	0.354	0.087
1-7	0.162	0.002	0.008	<0.001	0.140	0.760
1-8	0.002	0.003	<0.001	<0.001	0.035	0.723
2-3	0.099	0.030	0.004	0.011	<0.001	0.469
2-4	0.153	0.063	0.219	0.039	0.052	<0.001
2-5	0.002	0.358	0.031	0.016	0.018	0.010
2-6	0.178	0.685	<0.001	0.081	0.343	0.062
2-7	0.003	0.544	0.026	0.203	0.839	0.197
2-8	<0.001	0.018	0.002	0.129	0.118	0.072
3-4	0.866	0.079	0.804	0.001	0.716	0.119
3-5	0.034	0.934	0.012	0.102	0.001	0.139
3-6	0.100	0.551	0.209	0.596	0.214	0.307
3-7	<0.001	0.009	0.001	0.047	0.174	0.220
3-8	<0.001	0.001	<0.001	0.006	0.282	0.104
4-5	0.006	0.132	0.873	0.457	0.013	0.002
4-6	0.007	0.237	0.655	0.313	0.012	0.811
4-7	<0.001	0.406	0.020	0.847	<0.001	0.526
4-8	0.345	<0.001	0.135	0.002	0.526	0.075
5-6	0.054	0.004	0.102	0.194	0.003	0.215
5-7	0.007	0.606	<0.001	0.670	0.712	0.337
5-8	0.216	0.313	0.940	0.808	0.232	0.484
6-7	0.001	0.008	0.094	0.001	<0.001	0.018
6-8	0.752	0.481	0.002	0.837	<0.001	0.427
7-8	0.001	0.102	0.190	0.002	<0.001	0.408

Comparing the angulations, we observed significant differences when comparing PIC-T in four abutments of the maxillary arch and in six of the mandibular arch. When

comparing PIC–TD, there were in two maxillary and six mandibular, and when comparing TD–T, there were in two maxillary and one mandibular abutment (Table 8).

Table 8. *p* values of the comparisons of each of seven relative angulations for both arches with three different IOSs combination. Significant *p*-values highlighted with bold numbers.

Abutment Maxillary/ Mandibular	PIC vs. TRIOS		PIC vs. Maxillary/Mandibular		True Definition vs. TRIOS	
	Maxillary <i>p</i> -Value	Mandibular <i>p</i> -Value	Maxillary <i>p</i> -Value	Mandibular <i>p</i> -Value	Maxillary <i>p</i> -Value	Mandibular <i>p</i> -Value
26/46	-	-	-	-	-	-
25/45	0.425	0.070	0.158	0.772	0.571	0.070
23/43	0.070	0.002	0.348	<0.001	0.447	0.257
22/42	0.002	0.001	0.973	0.005	0.002	0.059
11/31	0.012	0.004	0.088	0.014	0.190	0.049
13/33	0.909	<0.001	0.350	<0.001	0.438	0.405
14/34	0.001	0.002	0.035	0.002	0.022	0.102
16/36	0.010	0.001	0.001	<0.001	0.066	0.716

4. Discussion

Based on the results of the present study, the three studied IOSs showed different precision when compared with the pre-established limits. Therefore, the first hypothesis was rejected. The precision of the systems T and TD decreased when the distance between the implants increased; this is consistent with multiple *in vitro* studies [3,21,39,55]. This was more evident for the distances than for the angles; however, the PIC system was not affected by the increasing distance. Therefore, the second hypothesis was partially rejected. The T and TD systems again showed different results depending on the arch, obtaining worse precision in the mandibular arch than in the maxillary. The PIC obtained similar results for both arches. Therefore, the third hypothesis was partially rejected.

Since this is an *in vivo* study, the accuracy cannot be evaluated because it is not possible to obtain a gold standard; however, it is possible to analyze the precision, and it provides useful information regarding the predictability and degree of variability of the different digital impressions. The purpose of analyzing the trueness and precision of the impression is to know whether the IOS can obtain a digital working cast to manufacture prosthetic structures with passive adjustment. This was completed without taking into account the possible errors of the rest of the CAD–CAM digital workflow [56].

One interesting debate continues about the tolerable range of acceptable misfit for our suprastructures. The literature is once again heterogeneous, both about how to assess passive fit as well as the tolerable ranges of the misfit. It would be very beneficial to specify the limit of misfit and, above all, under what parameters [53]. These limits can be established according to the three-dimensional variation of each implant, the distance between them, the individual and relative angulation, etc. [1,6,31,33]. Manzella et al. studied the effect of the three-dimensional and angular variation of a single implant in a structure with four and six implants. They established limits of 150 μm in the horizontal plane, 50 μm in the vertical, and 1 degree in the variation of the angulation [53]. More studies of this kind, in which the movements of all the implants involved in a suprastructure are combined, would be necessary, since it would be logical to think that the greater the number of implants, the lower the misfit tolerance for each segment. The acceptable misfit in the literature varies from 50 to 150 μm . The studies use different methodologies to measure the deviations, some report the data in the 3 axis (X, Y, Z), others with one single point evaluating distances and angles, and another very different methodology uses the best fit algorithm and compares the scanned Scanbodies. At the moment, there is no consensus of a clinically acceptable tolerance range [13,43]. In the present study, in order to help the reader interpret the results, the authors decided to select an arbitrary limit, based on the acceptable misfit published in previous articles. As the vast majority of studies are

carried out on four or six implants, and the present was eight, stricter limits were selected by reducing by half those described by Manzella [53]. The limit between two implants was placed at 75 μm for the distance and at 0.6 degrees for the relative angulation. In this way, the reader can see that if there was an established limit, the amount of times that the fit would not reach the limit, as a reference without affirming whether or not it has clinical relevance, since there is no such limit established in the literature yet.

In a multiple implant prosthesis, it is essential to study the Euclidean distances together with the angulations, since there are infinite angular positions of the abutments that can affect the fit of the structure even when they have the same distances [6,41]. In addition, we must analyze the precision/trueness, not only based on the data obtained by analyzing the mean deviation of the variables to study (distances or angulations), since these measurements compensate for one another, and the resulting data can hide or greatly minimize the errors, leading to situations in which almost no deviation is found, but when analyzing each variable individually, there are significantly more discrepancies [23] (Figure 9). As an example, when comparing the arithmetic means of the 28 Euclidean distances of the first and fifth impressions for the mandibular arch with the T system, a difference of 103 μm was obtained. However, when comparing each section individually, a difference of 167 μm was observed between Sections 1 and 5, 246 μm between 1 and 6, 317 μm between 1 and 7, and 477 μm between 1 and 8.

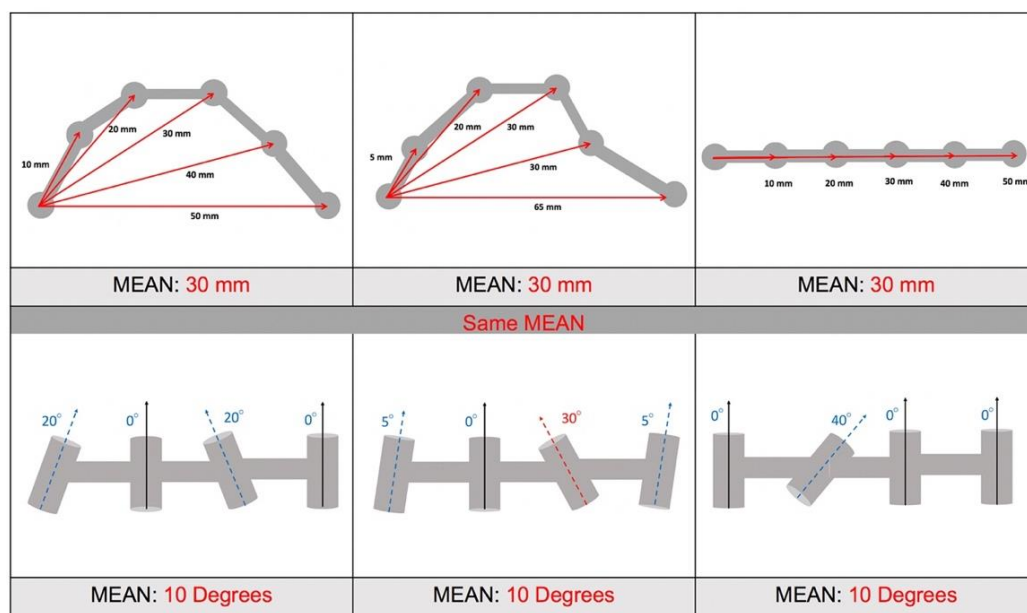


Figure 9. Analysis of trueness/precision calculated with each distance individually is more representative of real distortions than the means. See in the image that the same mean error can mean very different level of individual deviations, with very different clinical implications.

The comparison of 3D files using mesh alignment techniques (Best Fit) is used in many studies, since the process is relatively simple and gives a visual qualitative/quantitative idea of the discrepancies [7,8]. This process compensates for the discrepancies when the meshes align, as these do not share either the number, the size, or the distribution or form of triangles [21,30,32,33,57]. In addition, the results may be affected by the Best Fit algorithm used by each software, the alignment method, and above all by the amount of STL mesh that is selected in the process [31–33]. In the present study, the center points and rotational axes of the abutments of the suprastructures were calculated to analyze the precision of each scanner. The results would be the same as if performed on the measurements of the virtual replicas of the implants, since there is no virtual space between them; in this way, we have reached the last step of the CAD sequence. Every study contributes and increases knowledge, and it is subject to variations in its results due to errors and/or

differences in the instruments and software used, hence the need to standardize them and craft protocol [21].

According to van der Meer, all the intraoral scanners, including TD and T build their 3D models by combining several 3D images made of the same section of the model but from different angles. [14]. When the field of view decreases in size, the scan area increases, and more images are needed. Therefore, the scan protocol used and the starting point of the scan affect the precision of the impression. The images are stitched together by the algorithms that manage the scanner, increasing the definitive error when performing the 3D recomposition [21,31,42]. That is why our results agree with in vitro studies such as those of Gimenez, where this effect was already described [39,41,42,49]. As the scanner moves away from the starting point, there is an increasing pattern of imprecision. The standard error and the SD increase and, in particular, the maximum error between measurements. Another process that these two systems have to undergo is the transformation of the STL file to the digital working cast through the “Best Fit” alignment with the implant library in CAD design software. The effect of this step is proportional to the number of scan bodies that must be aligned. The PIC system lacks both steps, so when analyzing the data, it was observed that the error did not increase as we moved away from the starting point, in the way that happened in the other systems studied [42] (Figure 5). It is important to differentiate photogrammetry technology, in general, from the PIC system; they share similar physical principles, but in the PIC system, there is software linked to the cameras carrying specific algorithms adjusted to the oral environment [44–48].

The effect of the separation between implants and the consequent presence of edentulous areas are also factors, already described in the literature, that affect IOSs such as T and TD [9,37,42]. The lack of anatomical references for the soft tissues, added to the fact that the scan bodies used usually have the same exact design, causes the systems to lose the position when sewing the photos due to the lack of specific recognition areas [2,35]. The maxillary arch that has more keratinized tissue, along with the palate and its rugs can be factors that could help improve the impression precision [27,35]. In the present study, the authors think that another factor that could influence poorer results in the mandibular arch was the position of the eight implants. They presented less distance between them than in the maxillary arch; thus, it was challenging to scan interproximal areas of the scan bodies [2]. The PIC system was not affected by the arch type either, as shown in the results. As long as the two lenses can visualize the reference abutments and the rest of the PIC Transfers[®], the registration will be completed regardless of the soft tissue. In our case, it was achieved through small movements of the PIC camera[®], even though it is also possible to move the patient or rotate the PIC transfers (scan bodies) as needed.

The results, using the arbitrary limits selected, showed that the PIC system especially indicated for multiple implants cases had the best precision [43]. Another factor benefitting this system is that it does not depend on any scan pattern, therefore, being less sensitive to the operator [28]. On the other hand, TD performed second in precision but was the one more clearly affected by the increasing distance and had the disadvantage of using powder, even though as Kim et al. stated, systems that use powder are more accurate at happened in this study [21]. The T system was the one that obtained the worst precision data both in distances and in angulations, where it was more evident. It was observed by the authors, that the second impression of the mandibular arch was responsible for making the results worse. The operator had difficulties completing the impression following the scan pattern recommended by the manufacturer. This was not ruled out to avoid introducing any bias. On the other hand, it should be noted that T never offered its system for this type of treatment, specifying in its indications bridges on implants with a maximum of three pieces, where in different studies it obtained good results [21]. Despite the limitations of IOS for taking implant impressions, there are several clinical publications using IOS for a full arch already [58–65], and presentations showing these clinical cases performed with optical impressions are being regularly shown in dental congresses. That was one of the main reasons for comparing PIC with IOS in this in vivo study.

There are other variables that can influence the optical impression systems results; the type of implant connection being one of them, as well as the level at which the impression is taken (to an intermediate abutment or directly to the implant) as described previously in the dental literature, for conventional [66,67] as well as for optical impressions. Two systematic reviews of optical impressions mention these factors. Rütkunus et al. considered that these factors influenced the accuracy of optical impressions [2]. Zhang concluded that the type of connection and depth of the implants did not affect the accuracy [65].

The effect of the room light on IOS has been studied recently [68–70]. Studies show that it affected both mesh quality and accuracy, so room light must be adapted to each intraoral scanner. In the present study, the setting was a regular clinical room, and we followed the recommendations and instructions of the manufacturer that did not include any specifics about room light (just not to use the chair light).

A layer of titanium dioxide powder was needed in the True Definition IOS used in this study. The thickness of this layer has been calculated to be 20 to 40 microns and avoids light reflection [27]. Some authors, such as Nedelcu [71], state that this layer did not affect the final result of the impression. However, Rutkūnas [2] considered it to be a conditioning factor. Kim [21], in his study of the accuracy of nine intraoral scanners for complete-arch image acquisition, considered the IOS using this titanium dioxide powder the most accurate one, which was consistent with the results of this study.

As can be seen, there were significant differences ($p < 0.05$) between the Euclidean distances and angulations when comparing the scanners with each other [8,11]. This indicates that there is no reproducibility; that is, there is no precision between the IOS studied [8,11]. More in vivo studies are needed to evaluate whether optical printing systems can replace conventional impressions for this type of treatment. We propose studies with another number and distribution of implants, the use of other implant brands, as well as the use of intermediate abutments, different Scanbodies, different room lights, and IOSs with more developed software. For all this, the results of this study must be interpreted with caution.

5. Conclusions

Within the limitations of the present in vivo study, the following conclusions are drawn:

1. The system that obtained better precision was PIC, followed by TD, and then T.
2. The precision of T and TD decreased as the distance between the implants increased; however, this variable did not affect the PIC system.
3. The arch did not affect PIC precision, but the T and TD systems performed worse in the mandibular arch.

Author Contributions: Conceptualization, J.O.-P. and A.S.-L.; methodology, J.O.-P.; software, I.O.-C.; validation, J.O.-P., A.S.-L. and B.G.-G.; formal analysis, I.J.T.; investigation, J.O.-P.; resources, I.O.-C.; data curation, I.J.T.; writing—original draft preparation, J.O.-P.; writing—review and editing, B.G.-G.; supervision, A.S.-L.; All authors have read and agreed to the published version of the manuscript.

Funding: This research received no external funding.

Institutional Review Board Statement: The study was conducted in accordance with the Declaration of Helsinki and approved by the Institutional Ethics Committee of clinical research of Community of Madrid (TESISIMPLAN2014, 26 September 2014).

Informed Consent Statement: Informed consent was obtained from all subjects involved in the study.

Data Availability Statement: The data presented in this study are available on request from the corresponding author. The data are not publicly available due to privacy.

Acknowledgments: The authors thank MPI (Medical Precision Implants) for their materials, in terms of implant components, the DENTALMILL laboratory for their CAD/CAM supports, and Cristina Andreu for their help in preparing the formal analysis.

Conflicts of Interest: The authors declare no conflict of interest.

References

1. Flügge, T.; Meer, W.J.v.d.; Gonzalez, B.G.; Vach, K.; Wismeijer, D.; Wang, P. The accuracy of different dental impression techniques for implant-supported dental prostheses: A systematic review and meta-analysis. *Clin. Oral. Implant. Res.* **2018**, *29*, 374–392. [CrossRef] [PubMed]
2. Rutkūnas, V.; Gečiauskaitė, A.; Jegelevičius, D.; Vaitiekūnas, M. Accuracy of digital implant impressions with intraoral scanners. A systematic review. *Eur. J. Oral Implant.* **2017**, *10*, 101–120.
3. Mutwalli, H.; Braian, M.; Mahmood, D.; Larsson, C. Trueness and Precision of Three-Dimensional Digitizing Intraoral Devices. *Int. J. Dent.* **2018**, *2018*, 5189761. [CrossRef] [PubMed]
4. Kim, M.; Kim, J.; Lee, Y.; Lim, Y.; Lee, S. The effect of scanning distance on the accuracy of intra-oral scanners used in dentistry. *Clin. Anat.* **2019**, *32*, 430–438. [CrossRef] [PubMed]
5. Khraishi, H.; Duane, B. Evidence for use of intraoral scanners under clinical conditions for obtaining full-arch digital impressions is insufficient. *Evid. Based Dent.* **2017**, *18*, 24–25. [CrossRef]
6. Mangano, F.G.; Veronesi, G.; Hauschild, U.; Mijiritsky, E.; Mangano, C. Trueness and Precision of Four Intraoral Scanners in Oral Implantology: A Comparative in Vitro Study. *PLoS ONE* **2016**, *11*, e0163107. [CrossRef] [PubMed]
7. Imburgia, M.; Logozzo, S.; Hauschild, U.; Veronesi, G.; Mangano, C.; Mangano, F.G. Accuracy of four intraoral scanners in oral implantology: A comparative in vitro study. *BMC Oral Health* **2017**, *17*, 92. [CrossRef]
8. Renne, W.; Ludlow, M.; Fryml, J.; Schurch, Z.; Mennito, A.; Kessler, R.; Lauer, A. Evaluation of the accuracy of 7 digital scanners: An in vitro analysis based on 3-dimensional comparisons. *J. Prosthet. Dent.* **2017**, *118*, 36–42. [CrossRef]
9. Andriessen, F.S.; Rijkens, D.R.; Meer, W.J.v.d.; Wismeijer, D.W. Applicability and accuracy of an intraoral scanner for scanning multiple implants in edentulous mandibles: A pilot study. *J. Prosthet. Dent.* **2014**, *111*, 186–194. [CrossRef]
10. Joda, T.; Zarone, F.; Ferrari, M. The complete digital workflow in fixed prosthodont. *BMC Oral Health* **2017**, *17*, 124. [CrossRef]
11. Abduo, J. Accuracy of Intraoral Scanners: A Systematic Review of Influencing Factors. *Eur. J. Prosthodont. Restor. Dent.* **2018**, *26*, 101–121. [PubMed]
12. ISO-5725-1:1994 (E). Accuracy (Trueness and Precision) of Measurement Methods and Results—Part 1: General Principles and Definitions. International Organization for Standardization: Geneva, Switzerland ISO Store Order: OP-449776. 2018. Available online: <http://www.iso.org/iso/home.html> (accessed on 18 June 2020).
13. Katsoulis, J.; Takeichi, T.; Gaviria, A.S.; Peter, L.; Katsoulis, K. Misfit of implant prostheses and its impact on clinical outcomes. Definition, assessment and a systematic review of the literature. *Eur. J. Oral. Implant.* **2017**, *18*, 121–138.
14. Meer, W.J.V.d.; Andriessen, F.S.; Wismeijer, D.; Ren, Y. Application of Intra-Oral Dental Scanners in the Digital Workflow of Implantology. *PLoS ONE* **2012**, *7*, e43312.
15. Al-Meraikhi, H.; Yilmaz, B.; McGlumphy, E.; Brantley, W.; Johnston, W.M. In vitro fit of CAD-CAM complete arch screw-retained titanium and zirconia implant prostheses fabricated on 4 implants. *J. Prosthet. Dent.* **2018**, *119*, 409–416. [CrossRef] [PubMed]
16. Abduo, J. Fit of CAD/CAM Implant Frameworks: A Comprehensive Review. *J. Oral Implant.* **2014**, *40*, 758–766. [CrossRef] [PubMed]
17. Jemt, T.; Hjalmarsson, L. In Vitro Measurements of Precision of Fit of Implant-Supported Frameworks. A Comparison between “Virtual” and “Physical” Assessments of Fit Using Two Different Techniques of Measurements: Precision of Fit of Implant-Supported Frameworks. *Clin. Implant. Dent. Relat. Res.* **2012**, *14*, e175–e182. [CrossRef]
18. França, D.d.; Morais, M.; Neves, F.d.; Carreiro, A.; Barbosa, G. Precision Fit of Screw-Retained Implant-Supported Fixed Dental Prostheses Fabricated by CAD/CAM, Copy-Milling, and Conventional Methods. *Int. J. Oral Maxillofac. Implant.* **2017**, *32*, 507–513. [CrossRef]
19. Tsun, M.; Nicholls, J.; Rubenstein, J. Tolerance measurements of various implant components. *Int. J. Oral Maxillofac. Implant.* **1997**, *12*, 371–375.
20. Ortorp, A.; Jemt, T.; Bäck, T.; Jälevik, T. Comparisons of precision of fit between cast and CNC-milled titanium implant frameworks for the edentulous mandible. *Int. J. Prosthodont.* **2003**, *16*, 194–200.
21. Kim, R.J.-Y.; Park, J.-M.; Shim, J.-S. Accuracy of 9 intraoral scanners for complete-arch image acquisition: A qualitative and quantitative evaluation. *J. Prosthet. Dent.* **2018**, *120*, 895–903. [CrossRef]
22. Lee, S.; Lee, J. Digital Impressions for Implant-Supported Fixed Dental Prostheses. *Curr. Oral Health Rep.* **2017**, *4*, 136–141. [CrossRef]
23. Osnes, C.A.; Wu, J.H.; Venezia, P.; Ferrari, M.; Keeling, A.J. Full arch precision of six intraoral scanners in vitro. *J. Prosthodont. Res.* **2019**, *64*, 6–11. [CrossRef] [PubMed]
24. Ajioka, H.; Kihara, H.; Odaira, C.; Kobayashi, T.; Kondo, H. Examination of the Position Accuracy of Implant Abutments Reproduced by Intra-Oral Optical Impression. *PLoS ONE* **2016**, *11*, e0164048. [CrossRef] [PubMed]
25. Nedelcu, R.; Olsson, P.; Nyström, I.; Rydén, J.; Thor, A. Accuracy and precision of 3 intraoral scanners and accuracy of conventional impressions: A novel in vivo analysis method. *J. Dent.* **2018**, *69*, 110–118. [CrossRef] [PubMed]
26. Joda, T.; Ferrari, M.; Gallucci, G.O.; Wittneben, J.-G.; Brägger, U. Digital technology in fixed implant prosthodontics. *Periodontology 2000* **2017**, *73*, 178–192. [CrossRef]
27. Richert, R.; Goujat, A.; Venet, L.; Viguie, G.; Viennot, S.; Robinson, P.; Farges, J.-C.; Fages, M.; Ducret, M. Intraoral Scanner Technologies: A Review to Make a Successful Impression. *J. Healthc.* **2017**, *2017*, 8427595. [CrossRef]

28. Latham, J.; Ludlow, M.; Mennito, A.; Kelly, A.; Evans, Z.; Renne, W. Effect of scan pattern on complete-arch scans with 4 digital scanners. *J. Prosthet. Dent.* **2019**, *123*, 85–89. [[CrossRef](#)]
29. Medina-Sotomayor, P.; Pascual, M.A.; Camps, A.I. Accuracy of four digital scanners according to scanning strategy in complete-arch impressions. *PLoS ONE* **2018**, *13*, e0202916. [[CrossRef](#)]
30. Planitz, B.; Maeder, A.; Williams, J. The correspondence framework for 3D surface matching algorithms. *Comput. Vis. Image Underst.* **2005**, *97*, 347–383. [[CrossRef](#)]
31. Solaberrieta, E.; Otegi, J.R.; Goicoechea, N.; Brizuela, A.; Pradies, G. Comparison of a conventional and virtual occlusal record. *J. Prosthet. Dent.* **2015**, *114*, 92–97. [[CrossRef](#)]
32. Becker, K.; Wilmes, B.; Grandjean, C.; Drescher, D. Impact of manual control point selection accuracy on automated surface matching of digital dental models. *Clin. Oral Investig.* **2018**, *22*, 801–810. [[CrossRef](#)] [[PubMed](#)]
33. O'Toole, S.; Osnes, C.; Bartlett, D.; Keeling, A. Investigation into the accuracy and measurement methods of sequential 3D dental scan alignment. *Dent. Mater.* **2019**, *35*, 495–500. [[CrossRef](#)] [[PubMed](#)]
34. Mizumoto, R.M.; Yilmaz, B. Intraoral scan bodies in implant dentistry: A systematic review. *J. Prosthet. Dent.* **2018**, *120*, 343–352. [[CrossRef](#)]
35. Iturrate, M.; Eguiraun, H.; Etxaniz, O.; Solaberrieta, E. Accuracy analysis of complete-arch digital scans in edentulous arches when using an auxiliary geometric device. *J. Prosthet. Dent.* **2019**, *121*, 447–454. [[CrossRef](#)]
36. Treesh, J.C.; Liacouras, P.C.; Taft, R.M.; Brooks, D.I.; Raiciulescu, S.; Ellert, D.O.; Grant, G.T.; Ye, L. Complete-arch accuracy of intraoral scanners. *J. Prosthet. Dent.* **2018**, *120*, 382–388. [[CrossRef](#)] [[PubMed](#)]
37. Gan, N.; Xiong, Y.; Jiao, T. Accuracy of Intraoral Digital Impressions for Whole Upper Jaws, Including Full Dentitions and Palatal Soft Tissues. *PLoS ONE* **2016**, *11*, e0158800. [[CrossRef](#)] [[PubMed](#)]
38. Flügge, T.; Att, W.; Metzger, M.; Nelson, K. Precision of Dental Implant Digitization Using Intraoral Scanners. *Int. J. Prosthodont.* **2016**, *29*, 277–283. [[CrossRef](#)]
39. Giménez, B.; Özcan, M.; Martínez-Rus, F.; Pradies, G. Accuracy of a Digital Impression System Based on Active Triangulation Technology With Blue Light for Implants: Effect of Clinically Relevant Parameters. *Implant. Dent.* **2015**, *24*, 498–504. [[CrossRef](#)]
40. Fukazawa, S.; Odaira, C.; Kondo, H. Investigation of accuracy and reproducibility of abutment position by intraoral scanners. *J. Prosthodont. Res.* **2017**, *61*, 450–459. [[CrossRef](#)]
41. Giménez, B.; Özcan, M.; Martínez-Rus, F.; Pradies, G. Accuracy of a Digital Impression System Based on Parallel Confocal Laser Technology for Implants with Consideration of Operator Experience and Implant Angulation and Depth. *Int. J. Oral Maxillofac. Implant.* **2014**, *29*, 853–862. [[CrossRef](#)]
42. Gimenez-Gonzalez, B.; Hassan, B.; Özcan, M.; Pradies, G. An In Vitro Study of Factors Influencing the Performance of Digital Intraoral Impressions Operating on Active Wavefront Sampling Technology with Multiple Implants in the Edentulous Maxilla: Clinical Factors Influencing Intraoral Impression Performance. *J. Prosthodont.* **2017**, *26*, 650–655. [[CrossRef](#)] [[PubMed](#)]
43. Revilla-León, M.; Rubenstein, J.; Methani, M.M.; Piedra-Cascón, W.; Özcan, M.; Att, W. Trueness and precision of complete-arch photogrammetry implant scanning assessed with a coordinate-measuring machine. *J. Prosthet. Dent.* **2021**, *125*, S0022391321002808. [[CrossRef](#)] [[PubMed](#)]
44. Ortorp, A.; Jemt, T.; Back, T. Photogrammetry and Conventional Impressions for Recording Implant Positions: A Comparative Laboratory Study. *Clin. Implant. Dent. Relat. Res.* **2005**, *7*, 43–50. [[CrossRef](#)]
45. Stuardi, V.T.; Ferreira, R.; Manfredi, G.G.P.; Cardoso, M.V.; Sant'Ana, A.C.P. Photogrammetry as an alternative for acquiring digital dental models: A proof of concept. *Med. Hypotheses* **2019**, *128*, 43–49. [[CrossRef](#)] [[PubMed](#)]
46. Bergin, J.M.; Rubenstein, J.E.; Mancl, L.; Brudvik, J.S.; Raigrodski, A.J. An in vitro comparison of photogrammetric and conventional complete-arch implant impression techniques. *J. Prosthet. Dent.* **2013**, *110*, 243–251. [[CrossRef](#)]
47. Bratos, M.; Bergin, J.M.; Rubenstein, J.E.; Sorensen, J.A. Effect of simulated intraoral variables on the accuracy of a photogrammetric imaging technique for complete-arch implant prostheses. *J. Prosthet. Dent.* **2018**, *120*, 232–241. [[CrossRef](#)]
48. Revilla-León, M.; Att, W.; Özcan, M.; Rubenstein, J. Comparison of conventional, photogrammetry, and intraoral scanning accuracy of complete-arch implant impression procedures evaluated with a coordinate measuring machine. *J. Prosthet. Dent.* **2021**, *125*, 470–478. [[CrossRef](#)]
49. Giménez, B.; Özcan, M.; Martínez-Rus, F.; Pradies, G. Accuracy of a Digital Impression System Based on Active Wavefront Sampling Technology for Implants Considering Operator Experience, Implant Angulation, and Depth: Accuracy of Digital Impression Methods for Implants. *Clin. Implant. Dent. Relat. Res.* **2015**, *17*, e54–e64. [[CrossRef](#)]
50. Ciocca, L.; Meneghello, R.; Monaco, C.; Savio, G.; Scheda, L.; Gatto, M.R.; Baldissara, P. In vitro assessment of the accuracy of digital impressions prepared using a single system for full-arch restorations on implants. *Int. J. Comput. Assist. Radiol. Surg.* **2018**, *13*, 1097–1108. [[CrossRef](#)]
51. Guillermo, P.; Ferreira, A.; Özcan, M.; Giménez, B.; Martínez-Rus, F. Using stereophotogrammetric technology for obtaining intraoral digital impressions of implants. *J. Am. Dent. Assoc.* **2014**, *145*, 338–344.
52. Zeller, S.; Guichet, D.; Kontogiorgos, E.; Nagy, W.W. Accuracy of three digital workflows for implant abutment and crown fabrication using a digital measuring technique. *J. Prosthet. Dent.* **2019**, *121*, 276–284. [[CrossRef](#)] [[PubMed](#)]
53. Manzella, C.; Bignardi, C.; Burello, V.; Carossa, S.; Schierano, G. Method to improve passive fit of frameworks on implant-supported prostheses: An in vitro study. *J. Prosthet. Dent.* **2016**, *116*, 52–58. [[CrossRef](#)] [[PubMed](#)]

54. Jokstad, A.; Shokati, B. New 3D technologies applied to assess the long-term clinical effects of misfit of the full jaw fixed prosthesis on dental implants. *Clin. Oral Implant. Res.* **2015**, *26*, 1129–1134. [[CrossRef](#)] [[PubMed](#)]
55. Resende, C.C.D.; Barbosa, T.A.Q.; Moura, G.F.; Tavares, L.d.N.; Rizzante, F.A.P.; George, F.M.; Neves, F.D.d.; Mendonca, G. Influence of operator experience, scanner type, and scan size on 3D scans. *J. Prosthet. Dent.* **2021**, *125*, 294–299. [[CrossRef](#)] [[PubMed](#)]
56. Alghazzawi, T.F. Advancements in CAD/CAM technology: Options for practical implementation. *J. Prosthodont. Res.* **2016**, *60*, 72–84. [[CrossRef](#)] [[PubMed](#)]
57. Medina-Sotomayor, P.; Pascual-Moscardo, A.; Camps, I. Relationship between resolution and accuracy of four intraoral scanners in complete-arch impressions. *J. Clin. Exp. Dent.* **2018**, *10*, e361–e366. [[CrossRef](#)]
58. Sallorenzo, A.; Gómez-Polo, M. Comparative study of the accuracy of an implant intraoral scanner and that of a conventional intraoral scanner for complete-arch fixed dental prostheses. *J. Prosthet. Dent.* **2021**, *125*, S0022391321000834. [[CrossRef](#)]
59. Tohme, H.; Lawand, G.; Eid, R.; Ahmed, K.E.; Salameh, Z.; Makzoume, J. Accuracy of Implant Level Intraoral Scanning and Photogrammetry Impression Techniques in a Complete Arch with Angled and Parallel Implants: An In Vitro Study. *Appl. Sci.* **2021**, *11*, 9859. [[CrossRef](#)]
60. Rodríguez-Fernández, E.; Sánchez-Gil, A.; Maurice, S. Photogrammetry is Superior to Conventional Impression Techniques in Cases Requiring Six or More Implants. *EC Dent. Sci.* **2020**, *19*, 1–9.
61. Tohme, H.; Lawand, G.; Chmielewska, M.; Makhzoume, J. Comparison between stereophotogrammetric, digital, and conventional impression techniques in implant-supported fixed complete arch prostheses: An in vitro study. *J. Prosthet. Dent.* **2021**, *125*, S0022391321002699. [[CrossRef](#)] [[PubMed](#)]
62. Cappare, P.; Sannino, G.; Minoli, M.; Montemezzi, P.; Ferrini, F. Conventional versus Digital Impressions for Full Arch Screw Retained Maxillary Rehabilitations: A Randomized Clinical Trial. *Int. J. Environ. Res. Public Health* **2019**, *16*, 829. [[CrossRef](#)] [[PubMed](#)]
63. Chochlidakis, K.; Papaspyridakos, P.; Tsigarida, A.; Romeo, D.; Chen, Y.; Natto, Z.; Ercoli, C. Digital Versus Conventional Full-Arch Implant Impressions: A Prospective Study on 16 Edentulous Maxillae. *J. Prosthodont.* **2020**, *29*, 281–286. [[CrossRef](#)] [[PubMed](#)]
64. Albayrak, B.; Sukotjo, C.; Wee, A.G.; Korkmaz, İ.H.; Bayındır, F. Three-Dimensional Accuracy of Conventional Versus Digital Complete Arch Implant Impressions. *J. Prosthodont.* **2021**, *30*, 163–170. [[CrossRef](#)] [[PubMed](#)]
65. Zhang, Y.-J.; Shi, J.-Y.; Qian, S.-J.; Qiao, S.-C.; Lai, H.-C. Accuracy of full-arch digital implant impressions taken using intraoral scanners and related variables: A systematic review. *Int. J. Oral Implant.* **2021**, *14*, 157–179.
66. Papaspyridakos, P.; Hirayama, H.; Chen, C.-J.; Ho, C.-H.; Chronopoulos, V.; Weber, H.-P. Full-arch implant fixed prostheses: A comparative study on the effect of connection type and impression technique on accuracy of fit. *Clin. Oral Implant. Res.* **2016**, *27*, 1099–1105. [[CrossRef](#)]
67. Gracis, S.; Michalakis, K.; Vigolo, P.; Steyern, P.V.v.; Zwahlen, M.; Sailer, I. Internal vs. external connections for abutments/reconstructions: A systematic review. *Clin. Oral Implant. Res.* **2012**, *23*, 202–216. [[CrossRef](#)]
68. Revilla-León, M.; Jiang, P.; Sadeghpour, M.; Piedra-Cascón, W.; Zandinejad, A.; Özcan, M.; Krishnamurthy, V.R. Intraoral digital scans Part 1: Influence of ambient scanning light conditions on the accuracy (trueness and precision) of different intraoral scanners. *J. Prosthet. Dent.* **2019**, *124*, 372–378. [[CrossRef](#)]
69. Revilla-León, M.; Jiang, P.; Sadeghpour, M.; Piedra-Cascón, W.; Zandinejad, A.; Özcan, M.; Krishnamurthy, V.R. Intraoral digital scans Part 2: Influence of ambient scanning light conditions on the mesh quality of different intraoral scanners. *J. Prosthet. Dent.* **2019**, *124*, 575–580. [[CrossRef](#)]
70. Arakida, T.; Kanazawa, M.; Iwaki, M.; Suzuki, T.; Minakuchi, S. Evaluating the influence of ambient light on scanning trueness, precision, and time of intra oral scanner. *J. Prosthodont. Res.* **2018**, *62*, 324–329. [[CrossRef](#)]
71. Nedelcu, R.G.; Persson, A.S.K. Scanning accuracy and precision in 4 intraoral scanners: An in vitro comparison based on 3-dimensional analysis. *J. Prosthet. Dent.* **2014**, *112*, 1461–1471. [[CrossRef](#)] [[PubMed](#)]